Huang *et al.*
Chinese Journal of Mechanical Engineering (2023) 36:69
https://doi.org/10.1186/s10033-023-00900-x

Chinese Journal of Mechanical Engineering

ORIGINAL ARTICLE

Open Access

Allowance Extraction Considering of Inner and Outer Contour and Experimental Research on Belt Grinding of Hollow Blade

Yun Huang[1], Ming Wei[1], Guijian Xiao[1*], Shuai Liu[1] and Yuan Wu[1]

Abstract

Aero-engine fan blades often use a cavity structure to improve the thrust-to-weight ratio of the aircraft. However, the use of the cavity structure brings a series of difficulties to the manufacturing and processing of the blades. Due to the limitation of blade manufacturing technology, it is difficult for the internal cavity structure to achieve the designed contour shape, so the blade has uneven wall thickness and poor consistency, which affects the fatigue performance and airflow dynamic performance of the blade. In order to reduce the influence of uneven wall thickness, this paper proposes a grinding allowance extraction method considering the double dimension constraints (DDC) of the inner and outer contours of the hollow blade. Constrain the two dimensions of the inner and outer contours of the hollow blade. On the premise of satisfying the outer contour constraints, the machining model of the blade is modified according to the distribution of the inwall contour to obtain a more reasonable distribution of the grinding allowance. On the premise of satisfying the contour constraints, according to the distribution of the inwall contour, the machining model of the blade is modified to obtain a more reasonable distribution of the grinding allowance. Through the grinding experiment of the hollow blade, the surface roughness is below Ra0.4 μm, and the contour accuracy is between − 0.05~0.14 mm, which meets the processing requirements. Compared with the allowance extraction method that only considers the contour, the problem of poor wall thickness consistency can be effectively improved. It can be used to extract the allowance of aero-engine blades with hollow features, which lays a foundation for the study of hollow blade grinding methods with high service performance.

Keywords Double dimension constraints, Allowance extraction, Abrasive belt grinding

1 Introduction

With the development of aviation technology, the requirements of lightweight, high strength and high fatigue life are put forward for aero-engine fan blades [1, 2]. Wide-chord hollow fan blades become a key part of high bypass ratio turbofan engines for weight reduction [3, 4]. The weight reduction cavity inside the hollow blade has a very complex structure [5]. And the complex internal structure brings new influencing factors to the grinding of hollow fan blades. Since the internal structure of the blade cannot be reprocessed after forming, the consistency of the wall thickness of the hollow blade after processing is difficult to guarantee [6]. Therefore, considering the internal wall thickness of the blade grinding allowance extraction method is essential.

At the superplastic forming temperature, titanium alloy has good diffusion bonding performance, and the manufacture of titanium alloy hollow blades becomes possible [7]. Therefore, the superplastic forming and diffusion bonding (SPF/DB) process is a common method for manufacturing titanium alloy hollow blades with cavity structures [8]. Although SPF/DB technology appeared

*Correspondence:
Guijian Xiao
xiaoguijian@cqu.edu.cn
[1] College of Mechanical and Vehicle Engineering, Chongqing University, Chongqing 400044, China

in the United States in the 1970s [9], it is still a challenge for China to use this process to manufacture titanium alloy hollow blades. It is difficult to obtain the ideal shape in the design of the internal structure of the blade [10]. Starting from the microstructure of titanium alloy blades, Xun et al. [11] analyzed the wall thickness distribution of SPF/DB-formed blades and explained the causes of the uneven thickness distribution of hollow blades. The uneven wall thickness of hollow fan blades after hot forming is still a difficult problem to solve. In the grinding of hollow blades, the uneven wall thickness of the blade will make its consistency worse, which will affect the service performance of the blade. The influence of uneven wall thickness must be considered. So it is necessary to detect the inner contour of the blade.

Ultrasonic measurement is a common method for detecting the thickness of the inner wall of the cavity structure, which is often used to detect large-sized turbine fan blades or steel pipes [12, 13]. But for small and medium-sized and complex shapes of the blade, the use of ultrasonic measurement is difficult to detect, and ultrasonic measurement has a detection blind spot, the detection limit is limited [14]. Industrial Computer Tomography (ICT) is characterized by non-destructive testing and high measurement efficiency [15, 16]. The gray image obtained by X-ray through the blade can identify the inner contour of the blade and obtain the internal structure data of the blade [17]. Zeng et al. [18] proposed a detection method to compare ICT images with CAD models, which can realize the measurement and comparison of the internal structure of the blade, and has good automation and detection accuracy. Wang et al. [19] developed a high-precision CT measurement method, which can control the accuracy within 0.015 mm when measuring the blade wall thickness.

High-precision blade contour reconstruction is a key issue for the analysis and extraction of grinding allowance after obtaining blade contour information [20]. The NURBS curve interpolation method is often used to reconstruct the blade surface, which can effectively construct the blade surface [21, 22]. Peng et al. [23] proposed a multi-point cloud alignment method for complex-shaped blades, which can obtain more accurate information about the blade surface and obtain a better reconstruction model. After the model reconstruction is completed, it is necessary to find the optimal relative position between the reconstructed model and the design model, and establish constraints to measure the minimum distance between the model contours to obtain the distribution of machining allowance [24, 25]. Many matching methods use the ICP algorithm and its improved method [26, 27]. Xie et al. [28, 29] proposed an iterative variance-minimization matching (VMM) method, which can effectively avoid the influence of measurement defects on the matching process. Lv et al. [30] improved the VMM method by introducing a weighted variance so that the matching method has better robustness to negative and abnormal allowance. However, the research on the grinding allowance extraction method of hollow blades is mostly based on the outer contour, and the internal structure is rarely considered.

In order to obtain the appropriate grinding allowance distribution on the blade surface under the condition of considering the inner wall structure of the hollow blade, this paper proposes a method for extracting the grinding allowance of the hollow blade based on the double dimension constraints (DDC) of the inner and outer contours. Based on the blade contour and inner wall structure, considering the contact characteristics of the abrasive belt grinding process, the machining model of the hollow blade is modified to improve the wall thickness consistency of the blade and improve the service performance while meeting the contour accuracy requirements. Experiment results verify the validity and feasibility of the DDC method.

2 Method

2.1 Blade Re-construction Theory

Due to the large surface curvature change and complex structure of the titanium alloy hollow blade, it is difficult to use a three-coordinate measuring machine to measure it in contact, and it has a long measurement cycle. In this paper, blue light scanning is used to measure the contour of the blade, and the contour data of the blade to be processed is obtained. Blue light scanning can obtain a large amount of point cloud data on the blade surface in a short time, which greatly improves the detection efficiency of leaves, blue light scanning is easy to operate and lower requirements for operators. The device used is ATOS 5 airfoil blue light scanning device, which is used to measure the contour of the blade and obtain the surface data of the blade. The inwall thickness data inside the blade was scanned and detected by a high-energy industrial CT scanner of Chongqing Zhence Science and Technology Co., Ltd., and the scanning ray energy was 9Mev. The process of blue light detection and ICT detection is shown in Figure 1.

Before reconstructing the model, the point cloud data needs to be preprocessed, including cross-section layering, data denoising, and contour curve extraction. The point cloud data of the blade surface contour is defined as ($i=0,1\ldots m$; $j=0,1\ldots n$). Where m is the number of measurement points for a section, and n is the number of layers in the section. The surface measurement points P are distributed on the section plane perpendicular to the central axis of the blade, and the

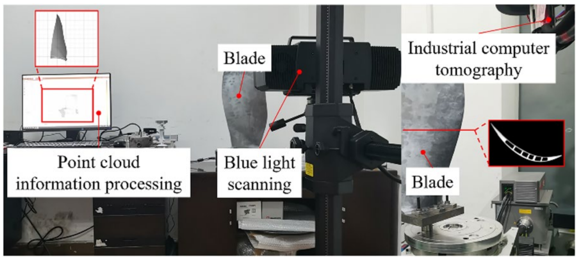

Figure 1 Blade detection process

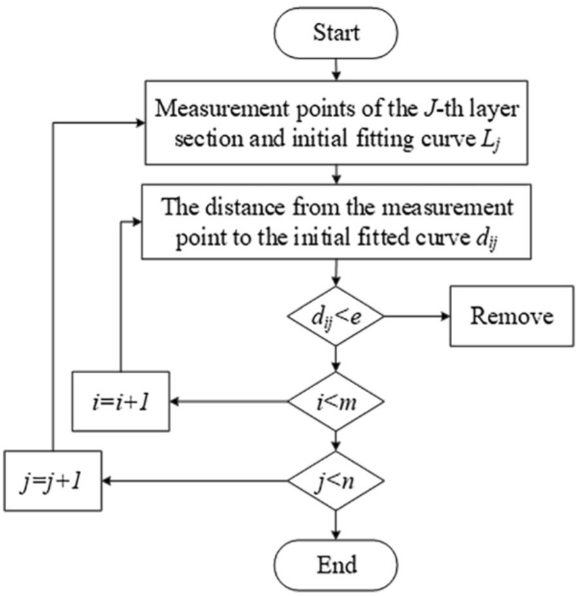

Figure 2 Noise reduction process

points on the same section have the same Z value. The noise reduction process is performed on the J-th layer section, and the redundant measurement points that are invalid in the section are removed. The process is shown in Figure 2, where e is the maximum allowable distance between the data point and the fitted curve.

In this paper, the method used for model reconstruction is the cross-section line lofting method. After the point cloud data is layered, the curve fitting is performed on the point cloud on each section to construct the contour curve on each section. The section line is lofted to reconstruct the complete blade surface to obtain the blade model. After denoising the points on the section, the NURBS curve interpolation method is used to fit the section contour. Fitting the section contour itself with seven arc constraints is the nearest estimation to the design data to obtain the best-fitting contour curve of the section [31]. Let the data point on the cross-section be $T_i(i=0,1...n)$, after noise reduction, and the NURBS curve obtained by fitting is *L(u)*, the following function can be obtained:

$$T_i = L(\overline{u_j}) = \sum_{j=0}^{n} \boldsymbol{D}_j R_{j,p}(\overline{u_j}), \quad j = 0, 1...n\,, \tag{1}$$

where $\boldsymbol{D}_j$ is the calculation control vertex; $R_{j,p}(u_j)$ is the basis function; u_j is the parameter of the curve; p is the degree of the spline.

In order to calculate the value of $\boldsymbol{D}_j$, it is necessary to determine the value of the basis function $R_{j,p}(u_j)$. The basis function $R_{j,p}(u_j)$ is defined as follows.

$$B_{j,p}(u) = \frac{\lambda_i N_{j,p}(u)}{\sum\limits_{j=0}^{n} \lambda_i N_{j,p}(u)}, \quad u \in [0,1]\,, \tag{2}$$

where λ_i is the weight factor; $N_{j,p}(u)$ can be obtained according to the De Boor-Cox recursive formula.

After obtaining the control point $\boldsymbol{D}_j$, start to construct the contour curve on the section, and bring in the NURBS surface definition formula to complete the NURBS surface interpolation reconstruction of the surface, and the reconstructed surface $S(u, v)$ is obtained as

$$S(u,v) = \frac{\sum\limits_{i=0}^{m}\sum\limits_{j=0}^{n} \lambda_{i,j} \boldsymbol{D}_{i,j} N_{i,p}(u) N_{j,q}(v)}{\sum\limits_{i=0}^{m}\sum\limits_{j=0}^{n} \lambda_{i,j} N_{i,p}(u) N_{j,q}(v)}, \tag{3}$$

where $\boldsymbol{D}_{i,j}$ is the control vertex, which is a topological rectangular array to form a control mesh; $\lambda_{i,j}$ is a weighting factor associated with vertex $\boldsymbol{D}_{i,j}$;$N_{i,p}(u)$, $i=0,1,...,m$ and $N_{j,q}(v)$ are the canonical B-spline basis of u-direction p-order and v-direction q-order, respectively.

The whole reconstruction process is shown in Figure 3. The point cloud model is obtained by measurement as shown in Figure 3(a). The point cloud data is then layered perpendicular to the Z-axis direction with the blade bottom surface as the initial plane. Each layer has a corresponding coordinate value on the Z-axis, and parallel sections are intercepted as shown in Figure 3(b). The NURBS curve interpolation method is used to fit the contour of the blade point cloud, and the contour curve of each section is obtained as shown in Figure 3(c). The obtained contour curve is arranged according to the corresponding z coordinate value, and it is lofted as Figure 3(d). The reconstructed blade model shown in Figure 3(e) can improve the reconstruction quality of the blade by increasing the number of sections.

The two models reconstructed based on blue light detection and ICT detection need to be registered to

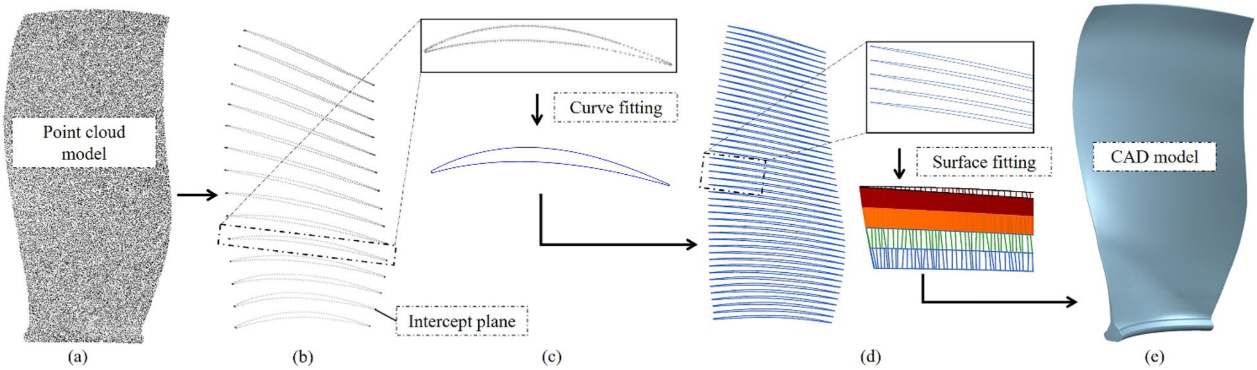

Figure 3 Blade reconstruction process: (**a**) Point cloud model obtained by measurement, (**b**) Section information extracted after delamination, (**c**) Fitting the extracted points using a b-spline curve, (**d**) Fitting the blade surface, (**e**) Reconstructed blade model

make them overlap into one, and a complete blade with contour and inwall thickness data is obtained. The registration alignment is performed by an iterative closest point (ICP) algorithm, which translates and rotates the two-part model to minimize the sum of squares between the points on the model surface to achieve the purpose of registration. The layering process uses a plane perpendicular to the Z-axis direction, so the corresponding parts of the two models have the same z-coordinate value. The model is registered without rotation around the X-axis and Y-axis and movement along the Z-axis. The coordinate transformation formula of the registration process is:

$$\begin{cases} x_i = \cos\gamma \cdot x_i' - \sin\gamma \cdot y_i' + l_x, \\ y_i = \sin\gamma \cdot x' + \cos\gamma \cdot y_i' + l_y, \\ \qquad z_i = c_i, \end{cases} \tag{4}$$

where γ is the angle of rotation around the Z-axis; l_x and l_y are the translations along the X-axis and Y-axis; $T_i(x_i, y_i, z_i)$ and $T_i(x_i^{'}, y_i^{'}, z_i^{'})$ are the coordinates before and after the transformation. Construct a function like the following:

$$f(\gamma, l_x, l_y) = \sum_i^n [(x_i - a_i)^2 + (y_i - b_i)^2 + (z_i - c_i)]. \tag{5}$$

The best registration between the two models is found by solving for the minimum of the function $f(\gamma, l_x, l_y)$. In order to make the obtained data more reliable, multiple iterations are performed on it to improve the reliability of the results. After the registration is completed, the two parts of the model are combined into a blade model containing the inner and outer contours, which is called the real blade model.

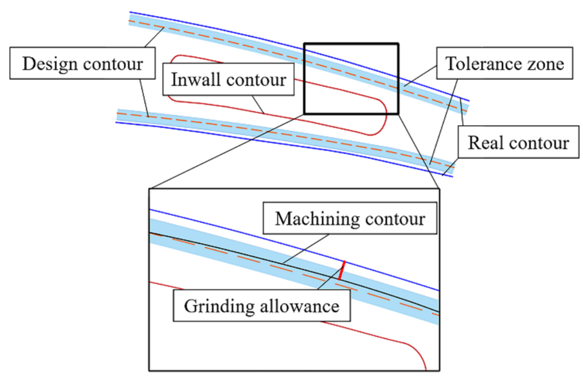

Figure 4 Grinding allowance extraction

2.2 Grinding Allowance Extraction Method Considering Inner and Outer Contours

There is enough margin on the blade surface to be machined, so before grinding the blade, it is necessary to obtain the margin distribution information on the blade surface. It is also necessary to register the reconstructed blade model with the design model. Suppose the real model and the design model are $P_i(i = 1, 2...n)$ and $X_i(i = 1, 2...n)$ respectively, and construct a rotation transformation matrix $\boldsymbol{R}$ and a translation transformation matrix $\boldsymbol{T}$. Through the iterative transformation of the matrices $\boldsymbol{R}$ and $\boldsymbol{T}$, the registration result is smaller than the preset value is solved. After the registration of the two models is completed, the grinding allowance of the blade surface is extracted.

According to the design model of the blade, the tolerance range of the blade contour is given, and the contour of the blade obtained after the final grinding process should be within the allowable tolerance range. On the basis of the contour constraint, the inwall contour constraint is proposed, and the outer contour line of the design model is changed according to the contour shape of the inwall to obtain a contour curve for machining as shown in Figure 4. This process is also carried out on the section plane, and the obtained machining contours are reconstructed into a model for grinding, which is called the machining model.

Calculate the normal vector of the contour curve of the inwall, and calculate the normal vector of the point on the section plane by calculating the least squares plane of a certain point on the curve. Calculate the neighborhood $Near(x_i)$ of a point x_i, which contains the m closest points of the point x_i, and find the covariance matrix:

$$CV = \sum_{x_j \in Near(x_i)} (x_j - x_i)(x_j - x_i)^{\mathrm{T}}, \tag{6}$$

where x_j is a point in the neighborhood $Near(x_i)$ of x_i, CV is a 3×3 positive semi-definite matrix, and the eigenvector $\boldsymbol{v}_i$ or $-\boldsymbol{v}_i$ corresponding to the minimum eigenvalue of CV can be used as the direction of the normal vector $\boldsymbol{n}_i$.

After the normal vector is obtained, the direction of the normal vector needs to be corrected so that the direction of the normal vector points outward. Take a point x_i and a point x_{i+1} adjacent to it, the tangent planes of the two points should be parallel, that is, $\boldsymbol{n}_i \cdot \boldsymbol{n}_j = \pm 1$, when the normal vector direction is consistent, $\boldsymbol{n}_i \cdot \boldsymbol{n}_j = 1$. And when $\boldsymbol{n}_i \cdot \boldsymbol{n}_j = -1$, the normal vector direction of one of the points needs to be corrected. Adjust the direction of the normal vector so that $\boldsymbol{n}_i \cdot \boldsymbol{n}_j = 1$ to complete the correction of the normal vector.

The distance along the normal vector direction between the contour of the inwall of the blade and the outer contour of the design model can be obtained, that is, the minimum distance. After calculating the distance between the inwall contour on the section plane and the outer contour of the design model, according to the calculated value and the variation trend of the blade wall thickness. Calculate the centroid of the inwall curve and offset the outer contour along the normal vector direction so that the centroid is located on the design contour. The weight ω is assigned to the offset curve, so that the changing trend of the curve is proportionally reduced within the given range, and the transition is smooth at the endpoint to obtain the modified contour curve, which is called the machining contour.

After completing the machining contour structure of each section cut in layers, the machining model of the blade is reconstructed. The machining model is compared with the design model, and the minimum distance between the contour of the machining model and the contour of the design model is calculated as the margin distribution of the blade surface. The obtained blade surface grinding allowance is shown in Figure 5, and the processing parameters are set according to the grinding allowance.

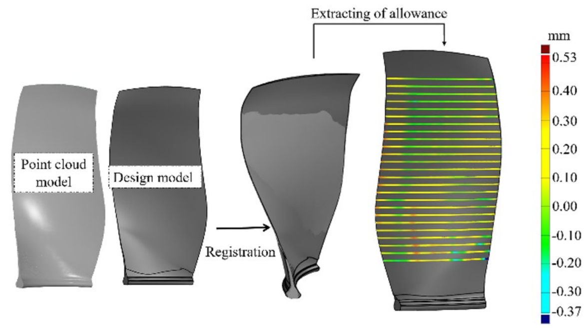

Figure 5 Grinding allowance distribution

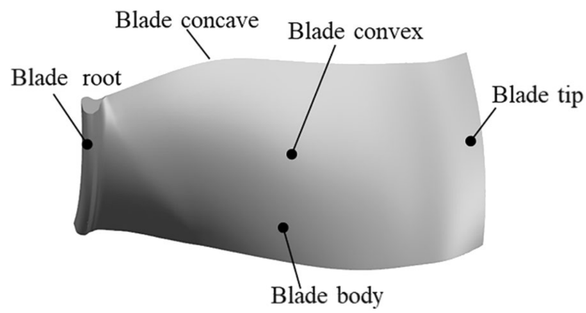

Figure 6 Blade model

3 Materials and Experiments

The blade used in the experiment is a hollow blade sample provided by China Aviation Development AECC Shenyang Liming Aero-Engine Co., Ltd. The sample is about 500 mm×250 mm×200 mm, which consists of a tenon and blade body. The thickness of the blade gradually increases from the blade tip to the tenon part, which has the characteristics of a wide chord and large torque, and the airfoil part has a cavity structure inside. The material of the blade is Ti-6Al-4V, and its model is shown in Figure 6.

The grinding experiment uses a seven-axis and six-axis linkage CNC grinding machine, and the grinding process of the blade is shown in Figure 7. The CNC grinding machine adopts Siemens CNC system to control the grinding process, and adopts a floating grinding head structure to ensure constant force grinding during the entire grinding process, and the blades are clamped on the turntable. The turntable has the movement of the *X*-axis, the *Y*-axis and the rotation of the *A*-axis, and the grinding head has the movement of the *Z*-axis and the rotation of the *B*-axis and the *C*-axis. The six movements are interlinked to realize the grinding of complex curved surfaces, especially the surface of the blade, which has the advantages of high efficiency,

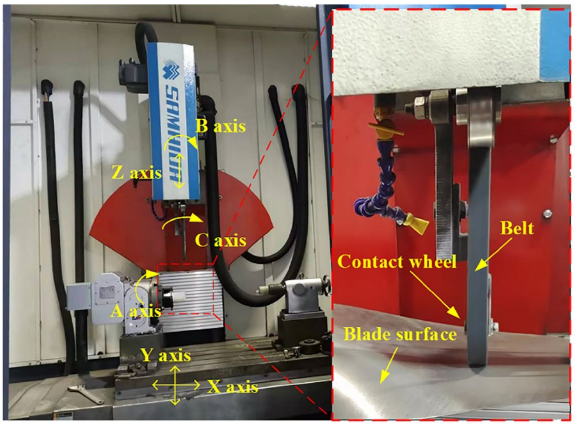

Figure 7 Precision CNC belt grinding experimental platform

Table 1 Blade grinding parameters

Parameters	Specification
Spindle speed (r/min)	2000
Feed speed (mm/min)	2400
Row spacing (mm)	0.72
Pressure depth (mm)	10
Belt size (mm^2)	2540*20
Belt type	Alumina hollow-sphere 545Y Nylon

stable grinding speed, high grinding precision and low cost. The grinding parameters are given in Table 1.

Before grinding the blade, it is necessary to set the technological parameters of the blade, and obtain the numerical control program required for the grinding process. Because the hollow blade has the characteristics of a wide chord and large torsion, the surface structure is complex. According to the main curvature distribution of the blade surface, the blade surface is divided into different processing areas. First, it is divided into two areas: the blade concave and the blade convex, and then each area can be divided into three parts: the blade tip, the blade body and the blade convex, a total of six areas. The blade tip vibrates the most during the grinding process, the blade body contains a cavity structure, and the blade root is the most difficult area to grind.

4 Results and Discussion

Modified on the basis of the design model, the machining model was obtained, and the surface grinding allowance of the hollow blade was extracted. In order to check whether the machining model obtained by the double dimensional constraints method can meet the machining requirements after being applied to the grinding of hollow blades, the surface roughness, contour and inwall structure of the blades after grinding were tested, and compared with the grinding allowance extraction method that only carries out the outer contour constraint.

4.1 Surface Roughness Analysis of Blade after Grinding

The detection of the blade surface is divided into three regions, namely the tip part, the blade body part and the blade root part. The blade tip part is the thinnest part of the entire blade, the blade body is the part containing the cavity structure, and the blade root part is connected with the tenon. Figure 8 shows the surface morphologies of different grinding areas after blade grinding.

It can be seen that after grinding, the surface roughness of all parts of the blade surface meets the processing requirements of $Ra<0.4$ μm. In the tip part, the average surface roughness is $Ra=0.284$ μm, and the average surface contour is $Rz=2.049$ μm. For the blade body, the average surface roughness is $Ra=0.235$ μm, and the average surface contour is $Rz=1.513$ μm. The average surface roughness of the blade root is $Ra=0.323$ μm, and the average surface contour is $Rz=2.135$ μm. When the blade is ground, it is cantilever clamping, and the blade tip part is away from the clamping end. There is a cavity structure in the airfoil part, and the surface morphology after grinding is complex. The blade root part is the most difficult part of the blade to process. When processing the blade root part, it is easy to cause interference between the grinding head of the machine tool and the turntable. The blade root is usually ground by restricting the rotation of the *B*-axis of the grinding machine, which results in a larger vibration during the grinding of the blade root, and the surface quality is not as good as that of the blade body and blade tip.

4.2 Analysis of the Wall Thickness of the Blade After Grinding

ICT inspection is performed on the blade after grinding. The inspection adopts a line array inspection that is different from the area array inspection before machining. Scanning inspection of a specific section inside the blade improves the accuracy of inspection and the efficiency of scanning. The cavity structure of the blade only exists in the blade body, so the ICT detection is only in the range containing the cavity structure. The whole cavity structure is divided into three regions, 15 dense sections are taken at the beginning and end of the blade cavity structure, and 15 sections are evenly distributed in the middle. Figure 9 shows the positions of 104 mm, 250 mm and 470 mm in the three regions. Figure 10 is the wall thickness data obtained using the two methods respectively.

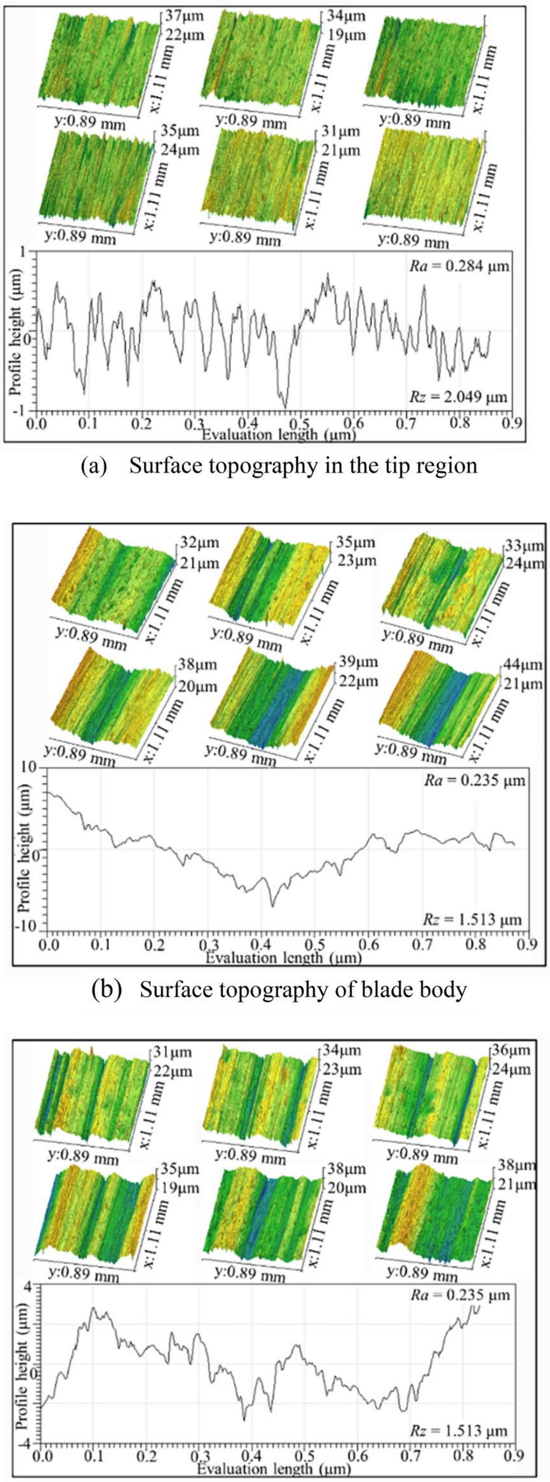

(a) Surface topography in the tip region

(b) Surface topography of blade body

(c) Surface morphology of blade root region

Figure 8 Surface morphology of blade after grinding

Compared with the blades ground by the classical ICP algorithm, that is, only considering the contour constraint method, the uniformity of the wall thickness of the blade obtained by the double size constraint algorithm is better, and the consistency of the wall thickness is significantly improved. The outer contour changes with the change of the inwall contour. Less allowance is extracted in the thin wall, and more allowance is extracted in the thicker. Considering the constraints of the contour, the processing method based on the double dimension constraint cannot obtain the inwall structure of the blade with the same wall thickness. However, compared with the processing without considering the constraints on the inwall contour, this method can make the wall thickness distribution of the blade more uniform and obtain better consistency. The experimental results show that the double-size constraint algorithm can obtain blades with better consistency and uniform wall thickness, and can extract the surface margin of the blade more effectively.

4.3 Comprehensive Analysis of Inner and Outer Contours Before and After Grinding

The detection results of blade contour after grinding are shown in Figure 10. The contour deviation of the blade tip part is 0.01–0.06 mm. Figure 11(a) shows the contour deviation of the blade tip on the convex of the blade, and Figure 11(b) shows the contour deviation of the blade tip on the blade concave. The contour deviation of the blade body is −0.04~0.13 mm. Figure 11(c) shows the contour deviation of the blade body on the convex of the blade, and Figure 11(d) shows the contour deviation of the blade body on the blade concave. The contour deviation of the blade root is − 0.02~0.04 mm. Figure 11(e) shows the contour deviation of the blade root on the convex blade, and Figure 11(f) shows the contour deviation of the blade root on the blade concave. The contour deviation of the blade body fluctuates greatly, because the cavity structure of the blade is inside the blade body, and the influence of the cavity structure is considered when processing the blade body part. After grinding, the contour deviation of the blade is within the tolerance range.

After data processing and rough matching, the grinding allowance distribution data and grinding results of the grinding allowance extraction method using the double dimension constraints method and the grinding allowance method which only analyzes the contour in the past are compared and analyzed. The difference between the two methods is whether the blade body contains the

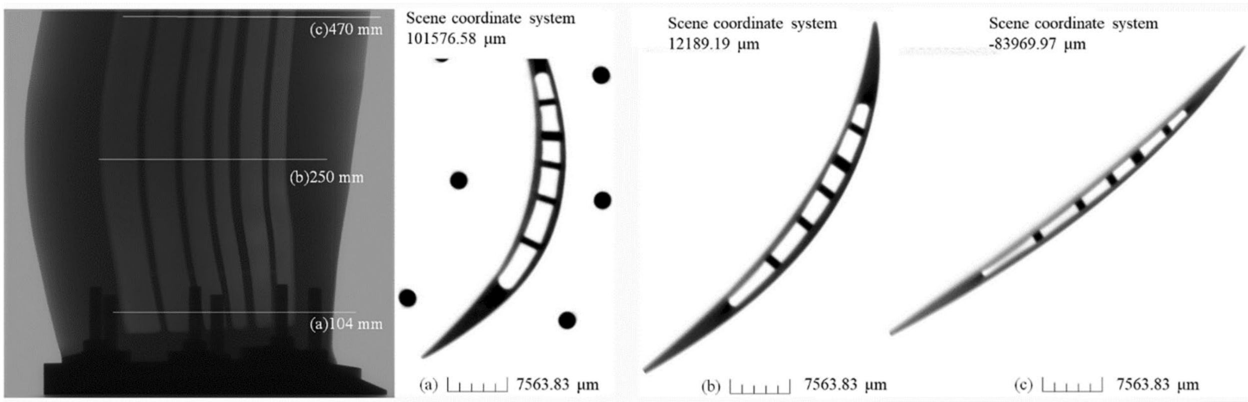

Figure 9 Wall thickness measurement of blades

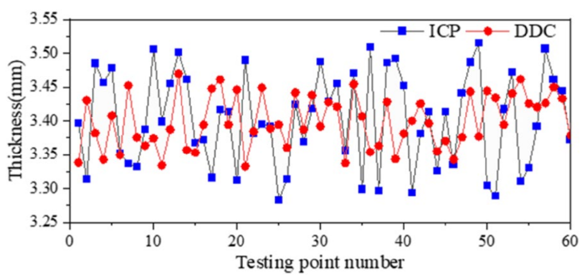

Figure 10 Wall thickness data of blades

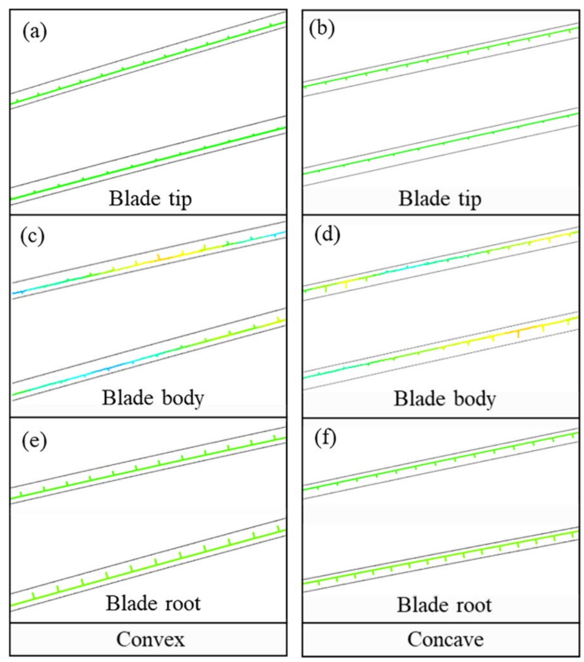

Figure 11 Contour detection (**a**) (**b**) detection results of blade tip, (**c**) (**d**) detection results of blade body (**e**) (**f**) detection results of blade root

cavity structure. The results of the section at a height of 250 mm.

Figure 12 shows the extraction of the surface grinding allowance of the hollow blade before grinding using the classical ICP algorithm and the double-size constraint algorithm, respectively. It can be seen from the comparison of the two figures that the classical ICP method does not consider the size constraints of the inwall thickness when calculating the grinding allowance, and the calculation of the allowance is carried out completely according to the constraints of the outline. Using the double dimension constraints method, the obtained grinding allowance value is related to the variation of the inwall thickness.

Figure 13 shows the deviation values of the blade surface contour after grinding the blade using the outer contour constraint method and the double dimension constraints method respectively. It can be seen from the figure that although both algorithms can be used to meet the processing requirements of the hollow blade contour, The deviation of the outer contour after grinding with the double dimension constraints method changes with the change of the inwall contour, and better wall thickness consistency can be obtained than that obtained by the outer contour constraint method.

Figure 14 shows the contour deviation detection of the blade on the 250 mm section plane. It can be seen that there is no cavity structure on the left and right sides of the blade, and the machining error of the blade shape is evenly distributed. At the cavity structure part, it can be seen that the deviation of the blade surface has a large float, which is the result of the correction according to the inner wall contour.

The distribution trend of the blade surface deviation is consistent with the contour of the inner wall, indicating

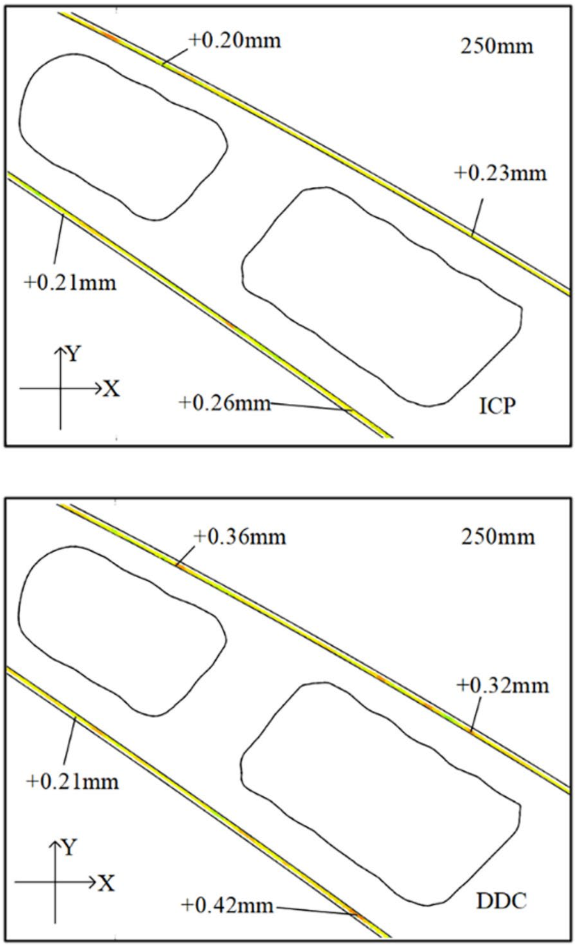

Figure 12 Schematic diagram of the contour allowance distribution obtained by two methods before grinding

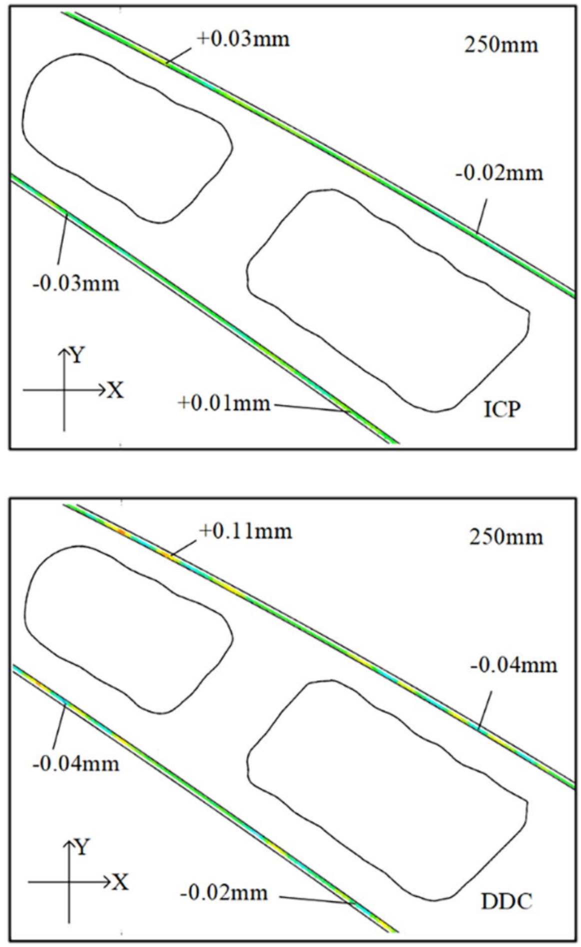

Figure 13 Schematic diagram of the contour allowance distribution obtained by two methods after grinding

that the correction of the contour of the machining model has obtained the desired results. Comparing the deviation distribution of the blade convex and the blade concave on the cross-section, it can be seen that the deviation of the blade concave part of the blade is smaller than that of the blade convex part, which is caused by the characteristics of the blade and the abrasive belt grinding. The contact area between the sand belt and the blade in the blade concave part is large, and the proportion of material removal is also enlarged. In the process of calculating the grinding allowance, it is necessary to further correct this part of the influencing factors.

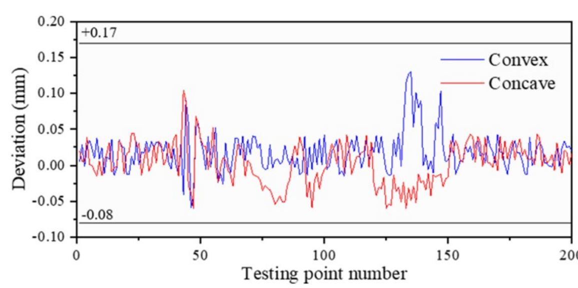

Figure 14 Deviation distribution

5 Conclusions

Based on the phenomenon of uneven wall thickness distribution and poor consistency caused by the difficulty in guaranteeing the inwall thermoforming accuracy during the manufacturing process of hollow blades, a method for extracting the grinding allowance of hollow blades based on the double dimension constraints of the inner and outer contours was proposed. The conclusions of the study can be summarized as follows:

(1) The blade model is reconstructed by the section line lofting method. Considering the contour of the blade and the inwall, the machining model of the hollow blade is modified the consistency of the blade and the uniformity of the wall thickness are improved under the premise of satisfying the contour accuracy.
(2) The surface roughness of the blade after grinding is between $Ra=0.20$ μm and $Ra=0.35$ μm, which meets the processing requirements. The contour deviation of the blade meets the processing requirements of − 0.08 ~ 0.17 mm.
(3) The internal and external contours and wall thickness after grinding are comprehensively analyzed. Compared with the method that only constrains the contour, the double dimension constraints method can reasonably allocate the grinding allowance on the surface of the hollow blade.
(4) Using this method to grind the blade not only meets the processing requirements of the blade surface contour, but also makes the thickness of the inner wall of the blade more uniform, and improves the problem of poor consistency of the hollow blade.

Acknowledgements
Not applicable.

Author contributions
YH wrote and modified the manuscript; MW wrote the manuscript and carried out experiments; GX was in charge of the whole research and modified the manuscript; SL and YW modified the manuscript and assisted with the experiments. All authors read and approved the final manuscript.

Authors' Information
Yun Huang, born in 1962, is currently a professor and a PhD candidate supervisor at *College of Mechanical and Vehicle Engineering, Chongqing University, China*. His main research interests include mechachonics engineering, belt grinding.
Ming Wei, born in 1998, is currently a master candidate *at College of Mechanical and Vehicle Engineering, Chongqing University, China.*
Guijian Xiao, born in 1986, is currently an associate professor and a PhD candidate supervisor at *College of Mechanical and Vehicle Engineering, Chongqing University, China*. His main research interests include mechachonics engineering, belt grinding.
Shuai Liu, born in 1996, is currently a PhD candidate at *College of Mechanical and Vehicle Engineering, Chongqing University, China.*
Yuan Wu, born in 1996, is currently a master candidate at *College of Mechanical and Vehicle Engineering, Chongqing University, China.*

Funding
Supported by National Natural Science Foundation of China (Grant No. U1908232), National Science and Technology Major Project (Grant No. 2017-VII-0002-0095).

Data availability
The datasets supporting the conclusions of this article are included within the article.

Declarations

Competing Interests
The authors declare no competing financial interests.

Received: 15 June 2022 Revised: 15 May 2023 Accepted: 16 May 2023
Published online: 09 June 2023

References
[1] Z M Chen, J B Liu. Fan/compressor aero design technology for high bypass ratio turbofan. *Acta Aeronautica et Astronautica Sinica*, 2008, 29(3): 513-526. (in Chinese)
[2] P B Zhao, Y Y Shi. Composite adaptive control of belt polishing force for aero-engine blade. *Chinese Journal of Mechanical Engineering*, 2013, 26(5): 998-996.
[3] Y Huang, C S Li, J G Xiao, et al. Research progress of aero-engine blade materials and anti-fatigue grinding technology. *Journal of Aeronautical Materials*, 2021, 41(4): 17-35. (in Chinese)
[4] X Zhou, H D Zhang, M Luo, et al. Toolpath dependent chatter suppression in multi-axis milling of hollow fan blades with ball-end cutter. *The International Journal of Advanced Manufacturing Technology*, 2014, 72(5/8): 643-651.
[5] L Jiang, Y H Wang, N S Shi, et al. Research on shape and position control during the forming of the different hollow blades with low melting point alloy mandrel. *International Journal of Advanced Manufacturing Technology*, 2022, 120(11-12): 7843-7853.
[6] Z H Zhang, Y Q Liang, T S Chen, et al. Research on adaptive belt grinding aeroengine titanium alloy fan blade. *Diamond & Abrasives Engineering*, 2018, 38(5): 67-72. (in Chinese)
[7] Z Huang, Z H Dong, W Z Zhou, et al. Modeling and prediction of grinding force on belt grinding TC4. *Surface Technology*, 2018, 47(9): 250-258. (in Chinese)
[8] N Wang, H M Chen, S L Xie. Hot flow behavior characterization for predicting the titanium alloy TC4 hollow blade surface Sinkage defects in the SPF/DB process. *International Journal of Material Forming*, 2019, 12(5): 827-844.
[9] Q X Han, H X Li, P X Bai. The key technical problems and quality control of titanium alloy two-layer large component SPF/DB. *Journal of Plasticity Engineering*, 2012, 19(4): 12-15. (in Chinese)
[10] C Z Zhao, H J Xu, C Y Fu, et al. An investigation on adaptively machining the leading and tailing edges of an SPF/DB titanium hollow blade using free-form deformation. *Chinese Journal of Aeronautics*, 2018, 31(1): 178-186.
[11] W Y Xun, J M Tan. Applications of superplastic forming and diffusion bonding to hollow engine blades. *Journal of Materials Processing Technology*, 2000, 99(s1-3): 80-85.
[12] G C Xu, Z P Ma, G D Xiao, et al. Robotic nondestructive testing technology for aero-engine blades. *Aeronautical Manufacturing Technology*, 2019, 62(14): 42-48. (in Chinese)
[13] K S Chakrapani, V Dayal, R Krafka, et al. Ultrasonic testing of adhesive bonds of thick composites with applications to wind turbine blades. *38th Annual Review of Progress in Quantitative Nondestructive Evaluation*, Univ Vermont, Burlington, July, 17–22, 2011, 1430: 1284–1290. https://doi.org/10.1063/1.4716366.
[14] X Wu, Y S Zhou, M H Zhang, et al. Research on ultrasonic dynamic gate technology for inspection of rotational parts with variable thickness. *China Measurement & Testing Technology*, 2018, 44(5): 103-107. (in Chinese)
[15] L F Liu, Q Chao, W W Wu, et al. Synchronous scanning mode of industrial computed tomography for multiple objects test. *Journal of X-Ray Science and Technology*, 2017, 25(2): 765-775.
[16] C Z Qi, J P Ni, W Jiang, et al. Linear array industrial computerized tomography quantitative detection method for small defects based on coefficients of variation. *Journal of Electronic Materials*, 2021, 50(4): 2066-2074.
[17] U Hampel, L Babout, R Banasiak, et al. A review on fast tomographic imaging techniques and their potential application in industrial process control. *Sensors*, 2022, 22(6): 2309.

[18] L Zeng, J H He, B Z Zhang. Comparison inspection between ICT images & CAD model based on edge extracting by neural networks. *Optics and Precision Engineering*, 2011, 19(10): 2533-2540. (in Chinese)
[19] N Y Wang, S S Shuai, F X Ren, et al. Sub-pixel high precision dimensional measurement method for aero-engine hollow turbine blade based on industrial computed tomography image. *China Foundry*, 2022, 19(4): 307-320.
[20] Y Z Jia, J F Wang, Q Y Wang, et al. Explicit correlation model of multi-source constraints for re-design parts with complex curved surface. *Chinese Journal of Mechanical Engineering*. 2014, 27(2): 385-391.
[21] D L Zhu, L B Yan, L Y Wang, et al. Inspection of blade profile and machining deviation analysis based on sample points optimization and NURBS knot insertion. *Thin-Walled Structures*, 2021, 162: 107540.
[22] H Ghorbani, F Khameneifar. Airfoil profile reconstruction from unorganized noisy point cloud data. *Journal of Computational Design and Engineering*, 2021, 8(2): 740-755.
[23] X W Peng, N Y Wang, H Zhang, et al. Stochastic joint alignment of multiple point clouds for contour blades 3-D reconstruction. *IEEE Transactions on Industrial Electronics*, 2022, 69(2): 1682-1693.
[24] J S Su, C Wang, K Chen, et al. MPCR-Net: Multiple partial point clouds registration network using a global template. *Applied Sciences-Basel*, 2021, 11(22): 10535.
[25] Q Z Zhu, T Z Chen, Y Zhang. A novel model reconstruction strategy for polishing turbine blade based on position optimization of sectional curve. *International Journal of Advanced Manufacturing Technology*, 2022, 119(7-8): 5011-5023.
[26] F J Liu, M X He, X Huang. An improved registration strategy for aligning incomplete blade measurement data to its model. *OPTIK*, 2021, 243: 167304.
[27] Y H Yu, G X Lyu, P Liu. Stream surface reconstruction of aero engine blade based on limited measured points. *Advances in Engineering Software*, 2019, 131: 90-101.
[28] H Xie, L W Li, P Z Yin, et al. Variance-minimization iterative matching method for free-form surfaces-part I: Theory and method. *IEEE Transactions on Automation Science and Engineering*, 2019, 16(3): 1181-1191.
[29] H Xie, L W Li, P Z Yin, et al. Variance-minimization iterative matching method for free-form surfaces-part II: Experiment and analysis. *IEEE Transactions on Automation Science and Engineering*, 2019, 16(3): 1192-1204.
[30] R Lv, D H Liu, J Z Wang, et al. WPMAVM: Weighted plus-and-minus allowance variance minimization algorithm for solving matching distortion. *Robotics And Computer-Integrated Manufacturing*, 2022, 76: 102320.
[31] K Mohaghegh, H M Sadeghi, A Abdulla. Reverse engineering of turbine blades based on design intent. *International Journal of Advanced Manufacturing Technology*, 2007, 32(9-10): 1009-1020.